THE JOURNAL OF BIOLOGICAL CHEMISTRY VOL. 288, NO. 4, pp. 2532–2545, January 25, 2013

RNA Targets and Specificity of Staufen, a Double-stranded RNA-binding Protein in *Caenorhabditis elegans*[*] [S]

Received for publication, July 3, 2012, and in revised form, November 27, 2012 Published, JBC Papers in Press, November 29, 2012, DOI 10.1074/jbc.M112.397349

Jacqueline Baca LeGendre[‡], Zachary T. Campbell[§], Peggy Kroll-Conner[¶], Phil Anderson[‖], Judith Kimble[§¶‖1], and Marvin Wickens[§2]

From the [‡]Graduate Program in Cellular and Molecular Biology, the [‖]Department of Genetics, the [§]Department of Biochemistry, and the [¶]Howard Hughes Medical Institute, University of Wisconsin, Madison, Wisconsin 53706

Background: Staufen binds and regulates structured mRNAs.
Results: *C. elegans* Staufen binds double-stranded RNAs *in vitro*. 418 putative mRNA targets have been identified. Mutants lacking a single RNA-binding domain enhance RNAi.
Conclusion: Staufen associates with target RNAs *in vivo*. *stau-1* mutants perturb RNAi.
Significance: RNA targets of Staufen are identified in an intact organism, and a connection between Staufen and RNAi is identified.

The Staufen family consists of proteins that possess double-stranded RNA-binding domains (dsRBDs). Staufen proteins of *Drosophila* and mammals regulate mRNA localization, translation, and decay. We report analysis of Staufen in *Caenorhabditis elegans*, which we have designated STAU-1. We focus on its biochemical properties, mRNA targets, and possible role in RNAi. We show that STAU-1 is expressed as mRNA and protein at all stages of *C. elegans* development. The wild-type, full-length protein, purified from bacteria, binds duplex RNA with high affinity *in vitro*. Purified, mutant proteins lacking single dsRBDs still bind RNA efficiently, demonstrating that no single domain is required for binding to duplex RNA (although dsRBD2 could not be tested). STAU-1 mRNA targets were identified via immunoprecipitation with specific anti-STAU-1 antibodies, followed by microarray analysis (RIP-Chip). These studies define a set of 418 likely STAU-1 mRNA targets. Finally, we demonstrate that *stau-1* mutants enhance exogenous RNAi and that *stau-1;eri-1* double mutants exhibit sterility and synthetic germ line defects.

Proteins specifically interact with mRNAs to regulate their movements and functions. These proteins recognize a diverse array of RNA-binding sites, ranging from single-stranded sequences to perfectly base-paired double-stranded elements (1). The RNA-bound proteins can control localization, translation, or stability of their mRNA targets (2). The double-stranded RNA (dsRNA)-binding protein, Staufen, participates in all three of these mRNA processes (3–5).

The dsRNA-binding proteins are a unique family of structurally related proteins that recognize RNA secondary structure (6). By definition, family members possess at least one dsRNA-binding domain (dsRBD),[3] which consists of an $\alpha\beta\beta\beta\alpha$ fold (7). A single protein can contain as many as five copies of this domain (6, 8). Multiple dsRBDs within a single protein enable cooperative RNA binding and stabilize the protein-RNA complex (8, 9). Individual dsRBDs are not identical; they exhibit different RNA binding and in some cases act as protein-protein interaction domains rather than RNA-binding domains (10). dsRBDs typically bind to duplex RNAs without dramatic sequence preference, via so-called "nonspecific" interactions. These interactions are most likely mediated through contacts with the RNA backbone rather than the nucleotide bases, as shown via NMR and crystallography (11–14). However, a single dsRBD binds a minimum length of dsRNA, which ranges from 11 to 16 base pairs (bp) (11, 12). *In vivo*, specificity for particular mRNAs is probably achieved through a combination of protein-RNA interactions and protein-protein interactions.

dsRNA-binding proteins exhibit diverse biological properties (15). Dicer plays key roles in the metabolism of small RNAs (16); ADAR (adenine deaminase acting on RNA) deaminates adenosine residues in its targets (17, 18); and PKR (double-stranded RNA-activated protein kinase) mediates cellular responses to duplex RNAs (19, 20).

RNA interference (RNAi) hinges on dsRNAs and therefore not surprisingly relies on multiple dsRNA-binding proteins (21–24). RNAi is a conserved mechanism initiated by dsRNA to suppress mRNA expression (25). The dsRNA trigger is processed to produce 21–25-nt small interfering RNAs (siRNAs), which guide the RNAi machinery to target mRNAs based on sequence complementarity (26). The pathway provides a defense against threats to the genome that utilize dsRNA (27–29).

Staufen, a dsRNA-binding protein composed of five dsRBDs, was initially identified in genetic screens for maternal effect

[*] This work was supported, in whole or in part, by National Institutes of Health Predoctoral Fellowship F31 GM084683 (to J. B. L.) and Grants GM095169 (to Z. T. C.), GM50933 (to P. A.), R01GM069454 (to J. K.), and GM031892 and GM050942 (to M. W.).

[S] This article contains supplemental Tables S1 and S2, Figs. S1–S5, and Data Sets 1–4.

[1] An investigator of the Howard Hughes Medical Institute.

[2] To whom correspondence should be addressed: 315B Biochemistry Addition, Dept. of Biochemistry, 433 Babcock Dr., Madison, WI 53706-1544. Tel.: 608-263-0858; Fax: 608-265-2603; E-mail: wickens@biochem.wisc.edu.

[3] The abbreviations used are: dsRBD, double-stranded RNA-binding domain; qRT-PCR, quantitative RT-PCR; IP, immunoprecipitation; SAM, significance analysis of microarrays; SAGE, serial analysis of gene expression; DAVID, Database for Annotation, Visualization, and Integrated Discovery; RACE, rapid amplification of cDNA ends; GO, gene ontology; SEQRS, *in vitro* selection, high throughput sequencing of RNA.

mutants in *Drosophila.* Staufen mutants exhibit multiple embryonic defects, including an absence of pole cells, abdomen reduction, and head deformation (30, 31). These defects are caused, at least in part, by mislocalization of mRNAs, such as *oskar* and *bicoid,* in the developing oocyte and embryo (32, 33). Staufen is also required for efficient localization of *prospero* mRNA during the formation of neuroblasts (10, 34). Staufen associates with the *bicoid* and *prospero* 3′-untranslated regions (UTR) *in vivo*. Staufen-mediated localization and binding to *bicoid* mRNA require a highly structured region in the *bicoid* 3′-UTR (33, 35, 36). Staufen is also required to derepress mRNAs after localization, implying additional functions in mRNA control (4).

Mammals possess two Staufen homologs, STAU1 and STAU2. Both proteins are present in neurons and located in ribonucleoprotein particles in dendrites (37–39). Staufen may facilitate transport of these particles to enable local translation at synapses (40, 41). The identity of Staufen mRNA targets in dendrites is not clear, but immunoprecipitation coupled with microarray analysis (RIP-Chip) identified candidate Staufen targets in cultured mammalian cells. In these experiments, STAU1 and STAU2 proteins were overexpressed in HEK293T cells, and thousands of transcripts were found to be associated with each protein (42). In addition, mammalian STAU1 promotes mRNA degradation by recruiting the nonsense-mediated decay factor, Upf1 (5). Together, the results with *Drosophila* and mammalian proteins thus imply functions in localization, translation, and decay.

Here, we identify and characterize the *Caenorhabditis elegans* homolog of Staufen, STAU-1. We purified full-length and mutant versions of STAU-1 protein and showed that all proteins bound dsRNA with high affinity. Mutant proteins lacking single dsRBDs that are otherwise full-length, still bind well, implying that no single domain is required for high affinity RNA interactions (although dsRBD2 could not be tested). Using STAU-1-specific peptide antibodies and RIP-Chip, we identify mRNA targets of endogenous STAU-1 protein. These STAU-1-associated mRNAs are diverse in function and show modest overlap with those identified in cultured mammalian cells. In addition, *stau-1* genetic mutants display enhanced RNAi phenotypes after exposure to dsRNA, and *stau-1;eri-1* double mutants have synthetic germ line defects that cause partial sterility.

EXPERIMENTAL PROCEDURES

Nematode Strains—N2 Bristol served as wild-type. All strains were grown at 20 °C on either NGM plates or S-basal liquid culture (see the WormBook Web site). None of the strains contained the *mut-16* mutation, which is present in many "wild-type" *C. elegans* backgrounds (43). The *stau-1(q798)* mutant was isolated from a deletion library generated by EMS mutagenesis (courtesy of the Barr laboratory). The library was screened by PCR using *stau-1*-specific primers. Positive pools were subdivided until the mutation was recovered in single animals (sib-selection). Progeny of individual animals carrying the mutation were further screened using multiplex PCR to identify homozygotes. *stau-1(q798)* deletes 1,384 bp of genomic sequence (beginning from the start codon, positions 4824–6207 are deleted) and removes exons 7 and 8 (strain ID JK4608). *stau-1(tm2266)* deletes 383 bp of genomic sequence (beginning from the start codon, position 4077–4459 is deleted) and spans from the middle of exon 5 to the middle of exon 6 (strain ID JK4607).

Analysis of Staufen mRNA—Total RNA was extracted from wild-type mixed stage worms using TriReagent (Sigma) and standard techniques. mRNA was isolated from total RNA using the PolyATract mRNA isolation system (Promega) and used for 5′- and 3′-rapid amplification of cDNA ends (RACE) via the FirstChoice RLM-RACE kit (Ambion). RACE PCR products were cloned into pCR II-TOPO vector (Invitrogen) and sequenced. The exon and intron boundaries for *stau-1,* F55A4.4, and F39E9.7 were verified by RT-PCR (see below). See supplemental Fig. S1 for additional sequence information.

Yeast Three-hybrid Assay—Full-length *stau-1* cDNA was cloned into pGADT7 (44) using the NdeI and XhoI sites (plasmid JB005). A random sequence generator (available on the University of California, Riverside, Web site) was used to create 23-bp dsRNAs (DS1–DS4). DNA oligonucleotides (see supplemental Table S2) corresponding to the dsRNA were cloned into the XmaI and SphI sites of pIIIa MS2–2 (DS1, plasmid JB029; DS2, plasmid JB030; DS3, plasmid JB031; DS4, plasmid JB026) as described previously (45).

The three-hybrid assay was performed using the YBZ-1 yeast strain, as described previously (45). RNA-protein interactions were assayed using the Beta-Glo System (Promega).

Protein Purification—Full-length *stau-1* cDNAs (wild-type or mutant) were cloned into a modified pGEX-4T-1 vector (GE Healthcare; wild-type, plasmid JB046; ΔdsRBD1, plasmid JB047; ΔdsRBD2, plasmid JB048; ΔdsRBD3, plasmid JB049; ΔdsRBD4, plasmid JB050; ΔdsRBD5, plasmid JB051), such that a His_6 tag is at the C terminus (gift from the Kimble laboratory). All constructs were cloned into the vector using XmaI and XhoI. Proteins were induced in BL21 (gold) cells (Stratagene) with 1 mM IPTG overnight at 16 °C. Cells were lysed in buffer (1× PBS, 10% glycerol, 20 mM imidazole, 0.5% Triton X-100, 300 mM NaCl, Complete protease inhibitors EDTA-free (Roche Applied Science), final pH 8.0), and proteins were bound to nickel resin (Qiagen) at 4 °C. Protein was eluted from resin with elution buffer (1× PBS, 30% glycerol, 250 mM Imidazole, final pH 8.0). The protein was further purified by binding to glutathione-Sepharose resin (Amersham Biosciences) in the presence of buffer (20 mM HEPES-KOH, pH 7.4, 0.5 M NaCl, 5 mM DTT, 0.02% Tween 20) at 4°C. The final sample was recovered from the resin with elution buffer (1× PBS, 30% glycerol, 50 mM glutathione, final pH 8.0).

Electrophoretic Mobility Shift Assay (EMSA)—Random sequence 3 dsRNA (DS3) was *in vitro* transcribed from DNA oligonucleotides using the MEGAscript T3 transcription kit (Ambion) and treated with alkaline phosphatase. The single-stranded RNA consisted of 23 nucleotides corresponding to one side of random sequence 3 (Dharmacon). All RNA was ^{32}P-end-labeled using T4 kinase. 2 fmol of RNA was combined with various protein concentrations (dsRNA was denatured and allowed to cool at room temperature for 30 min prior to incubation) in 10 mM HEPES (pH 7.4), 1 mM EDTA, 50 mM KCl, 2 mM DTT, 0.01% Tween 20, 0.1 mg/ml BSA, 10 units of RNase inhibitor, and 10 ng of yeast total RNA. Binding reactions were incubated for 30 min at room temperature in a total volume of 10 μl. Sample buffer (6% glycerol, 0.06% bromphenol blue) was

added to the reactions prior to loading on a prerun 5% Tris borate-EDTA-polyacrylamide gel (Bio-Rad). Samples were resolved on the gel for 35 min, 100 V at 4 °C and then exposed to a phosphorimager screen. Quantitation was performed on three replicas using ImageQuant (Amersham Biosciences) and GraphPad Prism 4 software. Antibody supershift EMSAs using purified STAU-1 were conducted as above with minor modifications. The two primary differences were the source of the RNA (commercially synthesized (IDT)) and the concentration of BSA in the binding reaction (increased 5-fold to 0.5 mg/ml). The concentration of STAU-1 was fixed at 50 nM. After the binding reaction was allowed to proceed, 1 μg of α-STAU-1 antibody was incubated with the reaction for 10 min at room temperature prior to electrophoresis for 45 min.

In Vitro Analysis of RNA Binding Specificity by in Vitro Selection, High Throughput Sequencing of RNA (SEQRS)—Full-length STAU-1 was purified as described using high capacity magnetic GST-agarose beads (Sigma-Aldrich) (46). Aliquots of protein were stored in 1× SEQRS buffer (50 mM Tris-HCl, pH 8, 0.1 mM $MgCl_2$, 150 mM NaCl, 0.1% Nonidet P-40) containing 20% glycerol prior to flash freezing and storage at −80°C. The SEQRS experiment was performed as described with minor modifications (47). Briefly, the initial libraries were transcribed from 1 μg of input dsDNA using the AmpliScribe T7-flash transcription kit (Epicenter). The reaction was treated with RNase-free DNase and purified using the GeneJET RNA purification kit (Fermentas). 150 ng of the purified RNA was added to 50−100 nmol of fusion protein corresponding to FBF-2, GST, or STAU-1 in a total volume of 100 μl. The samples were incubated for 30 min at ambient temperature prior to capture of the beads containing protein-RNA complexes via a 96-well magnetic block. The beads were washed four times with 200 μl of ice-cold SEQRS buffer. After the final wash step, the resin was resuspended in elution buffer (1 mM Tris, pH 8.0) containing 10 pmol of the reverse transcription primer. Samples were heated to 65 °C for 10 min and then cooled on ice. A 5-μl aliquot of the sample was added to a 10-μl ImProm-II reverse transcription reaction (Promega). The resulting ssDNA was used as a template for PCR. Prior to sequencing, the final PCR product was gel-purified following polyacrylamide gel electrophoresis. Approximately equal amounts of bar-coded DNA were combined based on individual concentrations determined by Quant-iT PicoGreen fluorescence assays (Invitrogen). After pooling samples, 3 pmol of DNA was sequenced on an Illumina HiSeq 2000 instrument using a custom primer. Sequences containing a bar code were identified using a custom MATLAB script (MathWorks). All measurements were normalized to account for differences in coupling efficiency during DNA synthesis.

Generation of STAU-1 Antibody—Rabbits were injected with peptide corresponding to amino acids 500–521 of STAU-1. Antibodies were purified using SulfoLink resin (Pierce) coupled to the same STAU-1 peptide used for antibody production. To determine antibody specificity, wild-type, *stau-1(q798)*, and *stau-1(tm2266)* mixed stage worms were resuspended in HB(A) buffer (50 mM HEPES, pH 7.6, 10 mM KCl, 1.5 mM $MgCl_2$, 0.2 mM EDTA, 0.5 mM EGTA, Complete protease inhibitors EDTA-free (Roche Applied Science), and 1 mM DTT), lysed using a mortar and pestle, and then homogenized. Lysate was then clarified by centrifugation, and the supernatant was dialyzed against HB(D) buffer (50 mM HEPES, pH 7.6, 10 mM KCl, 100 mM NaCl, 1.5 mM $MgCl_2$, 0.2 mM EDTA, 20% glycerol, 1 mM DTT). 20 μg of total protein for each strain was loaded on a 4–12% SDS gel, transferred to Immobilon-P membrane (Millipore), and incubated with purified STAU-1 antibody using standard Western techniques.

Isolation of Developmental Stages for qRT-PCR and Western Analysis—Wild-type gravid adults were digested with hypochlorite to release embryos. Embryos were allowed to hatch in S-basal liquid culture and grown at 20 °C. Each stage was harvested and used for subsequent analysis. Stages were verified based on germ line and vulval development visualized using a differential interference contrast microscope.

Immunoprecipitations—Wild-type and *stau-1(q798)* adults were resuspended in lysis buffer (50 mM Tris-Cl, pH 8, 150 mM NaCl, 3 mM DTT, 2 mM EDTA, 0.1% Nonidet P-40, 100 units/ml RNase inhibitor, and protease inhibitors (Roche Applied Science)) and lysed using sonication. Insoluble material was removed by spinning two times at 10,000 × *g* for 10 min at 4°C. Lysate was precleared with protein A-Sepharose (Sigma) for 1 h at 4°C. 6 mg of precleared extract was incubated with 20 μg of antibody (α-STAU-1 antibody or purified preimmune)/protein A-Sepharose for 2 h at 4°C while rotating. Protein A beads were then washed with 5 ml of lysis buffer, followed by four more washes with 1 ml of wash buffer (same as lysis buffer but without protease inhibitors and containing 10 units/ml RNase inhibitor). All washes were done at 4°C for 10 min while rotating. 10% of the beads were resuspended in 2× SDS sample buffer and boiled at 95°C for 5 min for Western analysis. The remaining beads were used for RNA extraction using TriReagent (Sigma). RNA was further purified using RNeasy Minelute columns (Qiagen). RNA quality of all samples was determined using a BioAnalyzer 2100 instrument (Agilent).

Microarrays—Preparation of RNA samples and hybridization to chips was performed by the University of Wisconsin-Madison Gene Expression Center. RNA samples were linearly amplified and biotin-labeled using the MessageAmp Premier RNA amplification kit (Ambion).

For IP samples, all of the amplified RNA for each sample was fragmented and hybridized to GeneChip *C. elegans* genome arrays (Affymetrix), which represent 22,500 transcripts, for each of three biological replicas. Each array was scaled according to control AFFX probe sets using the GeneChip Operating Software version 1.4 (Affymetrix) with a target intensity = 5,000. Data were filtered for probe sets called "present" in two of three wild-type α-STAU-1 IP samples. Filtered data were exported to Excel (Microsoft), $\log_2$-transformed, and mean-scaled within the sample replica. Differential enrichment between IP samples was determined using two-class paired significance analysis of microarrays (SAM) using the default number of permutations.

RT-PCR/qRT-PCR—Reverse transcription was carried out using random primers and Improm-II reverse transcriptase (Promega) using standard methods. cDNA was amplified using GoTaq Green Master Mix (Promega) and gene-specific primers. All primers crossed exon-exon boundaries to specifically amplify cDNA and not genomic DNA.

For qRT-PCR, reverse transcription was performed using random primers and Superscript II reverse transcriptase (Invitrogen). The TaqMan gene expression system (Applied Biosystems) was used for quantification of specific transcripts. TaqMan gene expression assays and Gene Expression Master Mix were used in a 7500 Fast Real-Time PCR machine. *ama-1* and *rps-25* were used as endogenous controls for normalization. Data were analyzed using the $\Delta\Delta C_T$ method (48). The following TaqMan assays were used: *stau-1*, Ce02491535_ml; *ama-1*, Ce02462726_ml; *rps-25*, Ce02464216_g1; *unc-70*, Ce02476754_m1; *cyd-1*, Ce02440641_m1; *vab-3*, Ce02499957 m1; *pha-4*, Ce02490534_m1.

Bioinformatics—Serial Analysis of Gene Expression (SAGE) data were obtained from the British Columbia *C. elegans* Gene Expression Consortium. Gene ontology classification was acquired using the Database for Annotation, Visualization, and Integrated Discovery (DAVID). Human homologs for *C. elegans* STAU-1 targets were identified using the Lund laboratory (University of Kentucky) microarray data set tools. *C. elegans* 3′-UTR sequences were downloaded from Biomart version WS220. Gibbs free energy values for 3′-UTRs were determined from predicted structures with the Mfold Quikfold application using energy rules RNA (version 3.0).

Scoring of Transgene Suppression—*stau-1(q798)* and *stau-1(tm2266)* males were mated to *qIs43* hermaphrodites. Strains were constructed such that F3 generation animals all contained the *qIs43* transgene but were homozygous, heterozygous, or wild-type for the *stau-1* mutation. F3 animals were singled onto plates and allowed to lay progeny and then removed and genotyped via PCR. Animals in the F4 generation were scored blindly based on their roller phenotype. We confirmed with PCR using primers specific to the transgene that non-roller and roller animals carried the transgene.

Enhancer of RNAi (Eri) Assay—Embryos for each strain were hatched on feeding RNAi plates (1 mM IPTG, 60 μg/ml carbenicillin, 50 μg/ml tetracycline) containing HT115 bacteria expressing *dpy-13* or *lir-1* dsRNA (constructs courtesy of the Kennedy laboratory). RNAi conditions were as described previously (49). Phenotypes were scored 5 days after exposure to RNAi as adults.

RESULTS

stau-1 Is a Staufen Homolog—The *C. elegans* genome encodes three genes related in sequence and architecture to *Drosophila* Staufen: F55A4.5 (hereafter *stau-1*), F55A4.4, and F39E9.7 (Fig. 1*A*). We found that all three genes generate RNAs detectable via RT-PCR (see supplemental Fig. S1 for sequences). To identify the 5′- and 3′-ends of the three transcripts, we performed 5′- and 3′-RACE. Both F55A4.4 and F39E9.7 contain early stop codons (Fig. 1*A*). These two genes are very similar at the nucleotide level (96% identical over 491 bp of genomic sequence, 46% identical overall), suggesting that they may have arisen from a recent gene duplication event. F55A4.4 and F39E9.7 generate endogenous siRNAs (43, 50, 51). In sum, F55A4.4 and F39E9.7 appear to be pseudogenes. The remaining Staufen-related gene, *stau-1* (F55A4.5), does not contain a premature termination codon, does not generate endogenous siRNAs, and possesses the biochemical characteristics of a Staufen protein (see below). We therefore consider STAU-1 to be the single Staufen homolog in *C. elegans.*

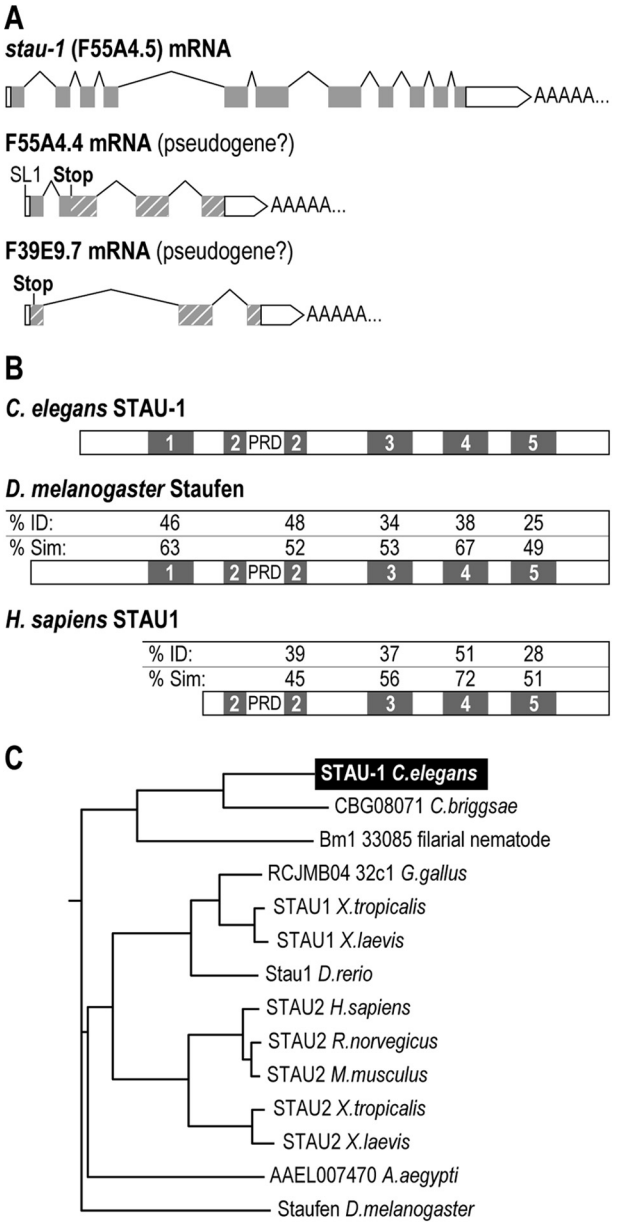

FIGURE 1. ***C. elegans stau-1* is a Staufen homolog.** *A*, exon and intron organization for *stau-1* (F55A4.5) and two likely pseudogenes, F55A4.4 and F39E9.7, as deduced from cDNAs. *White boxes* correspond to 5′- and 3′-UTRs, and *gray boxes* correspond to coding sequences. Introns are indicated by *lines* intersecting each exon. All three genes would potentially encode double-stranded RNA-binding proteins, but F55A4.4 and F39E9.7 contain early stop codons according to 5′-RACE analysis. F55A4.4 is SL1 transpliced. Transcripts for F55A4.4 and F39E9.7 are different than reported in WormBase version WS228 (See supplemental Fig. S1). *B*, protein domain structures for *C. elegans* STAU-1, *Drosophila melanogaster* Staufen, and *Homo sapiens* STAU1. The *numbered boxes* indicate double-stranded RNA-binding domains. *PRD*, proline-rich domain. Percentages indicate the percentage of identity and similarity (calculated according to the length of the shortest sequence) between *C. elegans* STAU-1 and the equivalent domain in the other species. The percentage of identity and similarity is only shown for the second half of domain 2, because there was little similarity for the first half of domain 2. *C*, a partial phylogenetic tree of Staufen homologs in different species. Full-length protein sequences from selected species were aligned using ClustalW. A phylogenetic tree based on the alignment was generated using the Phylip software package version 3.68.

The domain structure of STAU-1 protein is similar to that of *Drosophila* Staufen (Fig. 1*B*). Both the *C. elegans* and *Drosophila*

proteins contain five dsRBDs (7). Each of the STAU-1 dsRBDs is most similar to the corresponding domain in the other protein, as in other Staufens (Fig. 1*B*) (4). This supports the idea that each dsRBD has a distinct, conserved role. The *C. elegans* and *Drosophila* Staufens are unrelated in sequence outside the dsRBDs, with the exception of a proline-rich domain that interrupts dsRBD2. Over their entire lengths, the two proteins are only 26% identical, whereas the STAU-1 proteins of *C. elegans* and *Caenorhabditis briggsae* are 66.5% identical (Fig. 1*C*).

STAU-1 Binds Double-stranded RNA—To determine whether STAU-1 binds dsRNA, we utilized the yeast three-hybrid assay. A fusion protein composed of full-length STAU-1 and the Gal4 activation domain was expressed in yeast, together with a hybrid RNA consisting of a randomly generated sequence that forms a 23-bp stem (Fig. 2*A*). Binding of the STAU-1/Gal4 activation domain fusion protein to the RNA was expected to yield activation of a *LacZ* reporter; levels of β-galactosidase are well correlated with the affinity of protein-RNA interactions (45). Four dsRNAs

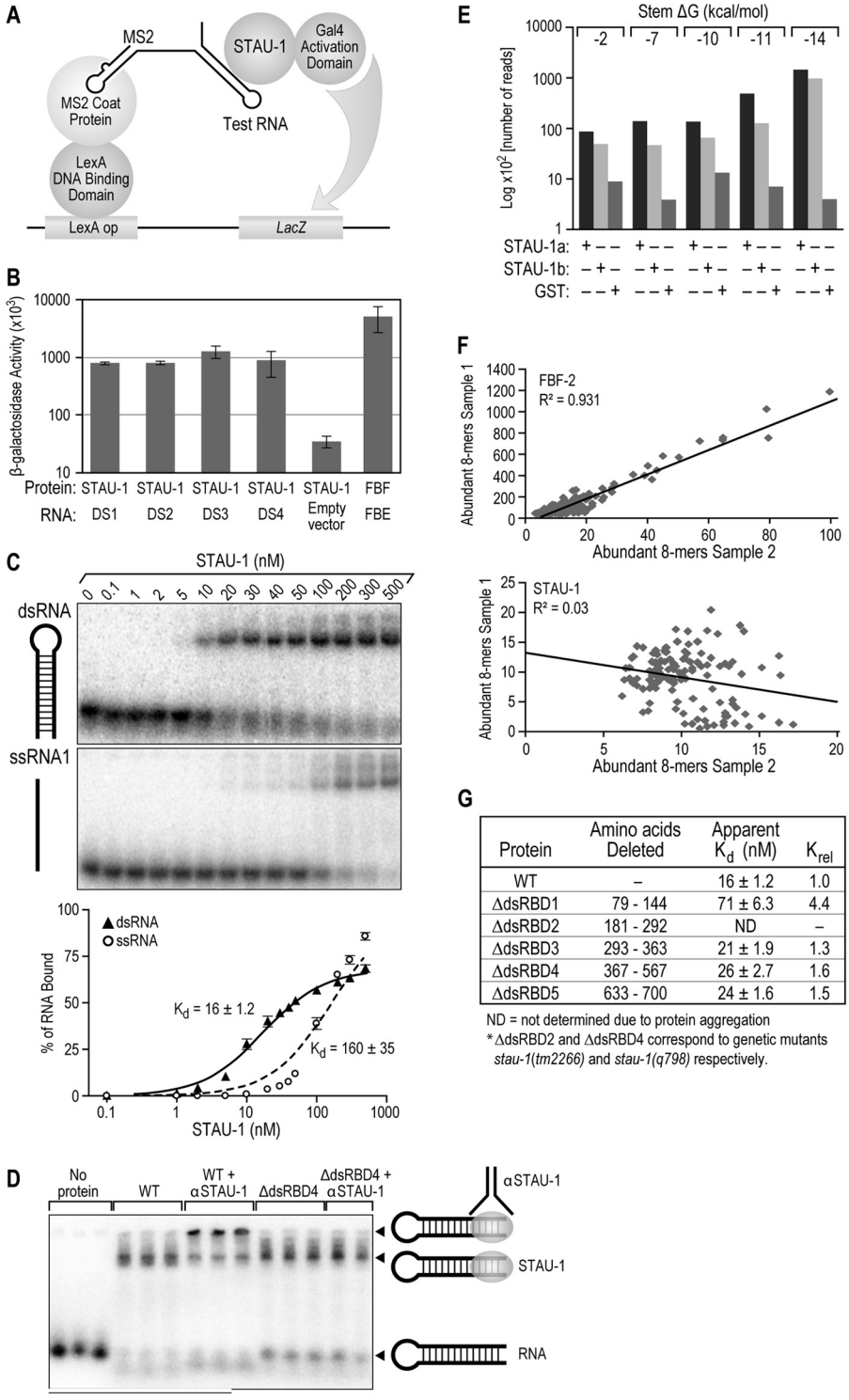

G

Protein	Amino acids Deleted	Apparent K_d (nM)	K_{rel}
WT	–	16 ± 1.2	1.0
ΔdsRBD1	79 - 144	71 ± 6.3	4.4
ΔdsRBD2	181 - 292	ND	–
ΔdsRBD3	293 - 363	21 ± 1.9	1.3
ΔdsRBD4	367 - 567	26 ± 2.7	1.6
ΔdsRBD5	633 - 700	24 ± 1.6	1.5

ND = not determined due to protein aggregation
* ΔdsRBD2 and ΔdsRBD4 correspond to genetic mutants *stau-1(tm2266)* and *stau-1(q798)* respectively.

(DS1–DS4), each with the same structure but a different sequence, were analyzed. STAU-1 bound all four 23-bp stems, and the affinities appeared comparable despite the fact that the sequences were unrelated (Fig. 2*B*). These results are consistent with other reports of Staufen binding dsRNA nonspecifically but with high affinity *in vitro* (12).

We next purified full-length STAU-1 protein containing a GST and His_6 tag (supplemental Fig. S2) and tested its binding biochemically to labeled RNAs *in vitro*. Bacterially expressed STAU-1 protein was first tested with DS3, a dsRNA that had been used in the three-hybrid assays. In electrophoretic mobility shift assays, STAU-1 bound DS3 with an apparent K_d of 16 nM (Fig. 2*C*), similar to the affinity of full-length human Staufen for dsRNA (K_d = 10 nM) (52). We also tested STAU-1 binding to single-stranded RNA that corresponded to one or the other side of the DS3 stem to determine whether the protein is specific for RNA secondary structure. STAU-1 bound 10-fold more weakly to the single-stranded RNA compared with the intact DS3 dsRNA (Fig. 2*C* and supplemental Fig. S3). (These experiments included EDTA and yeast tRNA to increase resolution, so binding affinities are not exact but still reflect relative affinities.) We confirmed binding of STAU-1 to dsRNA using antibody supershift assays (Fig. 2*D*). Both STAU-1 and a mutant of STAU-1 (ΔdsRBD4) bound the ^{32}P-labeled dsRNA (DS3 from Fig. 2*B*), resulting in slower migrating STAU-1·RNA complexes. The mutant protein lacks the target epitope recognized by the α-STAU-1 antibody (see Fig. 3*A*). In the presence of the antibody, the STAU-1·RNA complex migrated more slowly in samples containing the wild-type but not the mutant STAU-1 protein. The appearance of this "supershifted" species only with wild-type STAU-1 strongly suggests that STAU-1 (and not a contaminant in the preparation) is associated with the dsRNA. We conclude that STAU-1 binds tightly and preferentially to dsRNA.

STAU-1 Preferentially Binds Highly Structured RNAs in Vitro—To further characterize the binding specificity of STAU-1, we used a method termed SEQRS *(in vitro* selection, high throughput sequencing of RNA) (47). In this method, reiterated rounds of selection from RNA pools are followed by deep sequencing. The number of reads obtained correlates with independent measures of binding affinity (*i.e.* electrophoretic mobility shift and yeast three-hybrid assays) (47).

The starting material for our experiments consisted of DNA oligonucleotides, encoding five different structured RNAs with different length stems and five nucleotide loops, together with a mixture of random 20-mer sequences. The five structured RNAs varied in stem length from 4 to 10 base pairs and in Δ*G* from −2 to −14 kcal/mol. After transcription using T7 RNA polymerase, the resulting pool of RNAs was incubated with purified full-length STAU-1 protein immobilized on magnetic resin. After repeated washing, bound RNAs were thermally eluted and converted into double-stranded DNA using reverse transcription followed by PCR. This enrichment procedure was repeated for five cycles. The final pool was submitted for high throughput sequencing, and the relative amounts of each sequence were calculated.

Two separate preparations of STAU-1 protein enriched structured RNAs (Fig. 2*E*; the two preparations are referred to as STAU-1a and -1b). The enrichment of the structured RNAs correlated with the predicted stability of the RNA. Enrichment was specific for STAU-1 protein, because it was not observed with GST alone.

To determine whether STAU-1 bound specifically to single-stranded RNAs, we examined enrichment of the most abundant 8-mer sequences in each sample (Fig. 2*F*). All possible 8-mer sequences were extracted from the 20-mer data and sorted in order of frequency. As a control, we used *C. elegans* FBF-2, a protein known to bind single-stranded RNAs sequence-specifically. In two experiments using FBF-2, the most abundant 8-mers were well correlated, as expected, and reflected the protein's known binding site (R^2 = 0.931 (47)). In contrast, no such correlation was seen with STAU-1 (R^2 = 0.03). These data demonstrate that STAU-1 fails to bind single-stranded RNA in a reproducible, sequence-specific manner. However, it does bind double-stranded RNAs, with affinities that increase progressively with the stability of the stem.

Single dsRBDs Are Not Essential for Binding Double-stranded RNA—To determine whether any single STAU-1 dsRBD is essential for binding dsRNA, mutant proteins containing a GST and His_6 tag were purified and tested with DS3 RNA in electro-

FIGURE 2. **STAU-1 binds double-stranded RNA.** *A*, schematic for the yeast three-hybrid system. Full-length STAU-1 was fused to the Gal4 activation domain. An RNA hybrid was constructed between MS2 RNA and a double-stranded RNA stem-loop (DS1–DS4). STAU-1 binding to the double-stranded RNA stem-loop causes the Gal4 activation domain to come into close proximity to the LexA DNA binding domain, resulting in *LacZ* reporter expression. *LacZ* reporter expression indirectly measures the binding affinity of a protein for RNA but has been confirmed to directly correlate with the K_d (45). *B*, yeast three-hybrid results with full-length STAU-1 and double-stranded RNA stem-loops consisting of the same structure but possessing different RNA sequences (DS1–DS4). STAU-1 and empty vector (which contained no insert) served as a negative control. FBF protein and the FBE RNA served as a positive control. *C*, electrophoretic mobility shift assays with full-length STAU-1 and DS3 double-stranded RNA (*top*) or STAU-1 and single-stranded RNA (*ssRNA1*) consisting of the same sequence as one side of DS3 (*middle*). Binding curves (*bottom*) of STAU-1 affinity for double-stranded RNA and ssRNA1 indicate that STAU-1 binds double-stranded RNA with higher affinity (K_d = 16 ± 1.2) than single-stranded RNA (K_d = 160 ± 35). *D*, supershift assays with DS3 double-stranded RNA and STAU-1 or ΔdsRBD4 protein. The ΔdsRBD4 protein served as a negative control because it lacks the epitope recognized by the α-STAU-1 antibody. Two to three replicates of each experiment are shown. The STAU-1 protein preparations used here exhibited an A_{260}/A_{280} ratio of 0.50 (wild-type) and 0.52 (ΔdsRBD4), indicating that they were largely free of nucleic acids. *E*, analysis of STAU-1 specificity for RNA structure *in vitro*. The binding of full-length STAU-1 to double-stranded RNAs of variable sequence was determined following five rounds of selection using the SEQRS method (47). In these experiments, the number of reads correlates with binding affinity. Two preparations of STAU-1 (referred to as STAU-1a and -1b) enriched for structured RNAs of increasing stability; GST alone did not. RNA stability was calculated using the Vienna RNA structure algorithm (72). *F*, STAU-1 does not preferentially enrich for a single-stranded RNA motif. Following five rounds of selection, all possible 8-mer sequences were extracted from the library of random 20-mer sequences and compared across replicates. The 300 most abundant sequences were compared for STAU-1 and *C. elegans* FBF-2 (which binds single-stranded RNA in a sequence-specific manner, serving as a positive control). Enrichment was highly reproducible for FBF-2 (R^2 = 0.931) but not for STAU-1 (R^2 = 0.03). *G*, mutant versions of STAU-1, in which one double-stranded RNA-binding domain was deleted, were tested in electrophoretic mobility shift assays with DS3 double-stranded RNA. Boundaries of the deletions were designed based on the predicted extents of the dsRBDs as determined from protein alignments with *Drosophila* Staufen. For dsRBD2 and dsRBD4, the deletions corresponded to *C. elegans* mutants that delete each domain in the endogenous protein; these deletions remove all of the dsRBD plus small segments to either side. The dsRBD2 deletion mutant (ΔdsRBD2) could not be tested due to protein aggregation. *Error bars*, S.D.

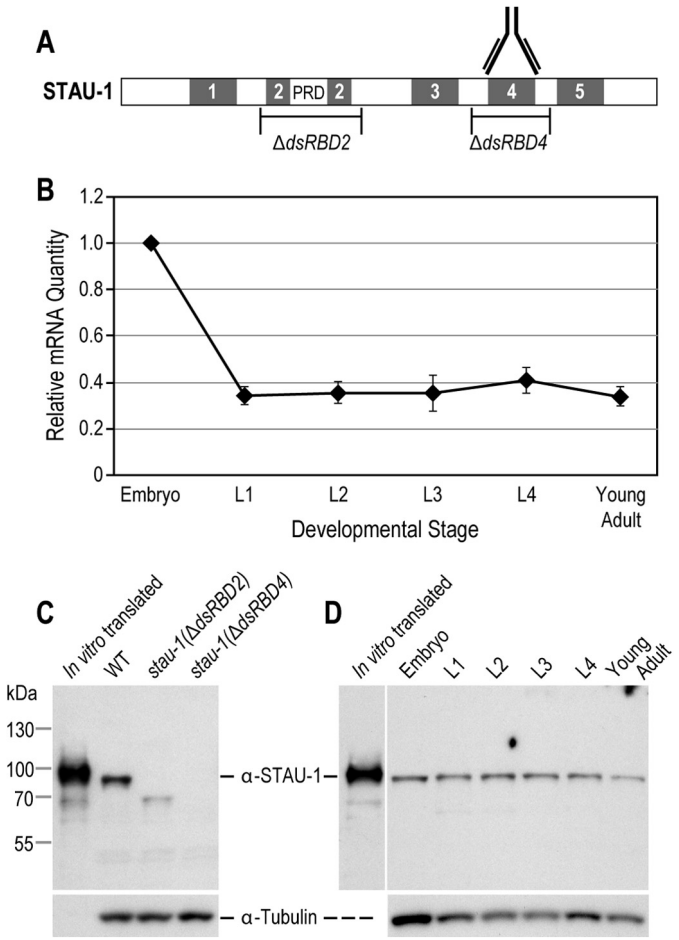

FIGURE 3. ***stau-1* is expressed throughout development.** *A*, domain structure of STAU-1 protein. *Brackets* indicate regions deleted in *stau-1* mutant alleles; *stau-1(tm2266)* deletes double-stranded RNA-binding domain 2 (referred to as *stau-1(ΔdsRBD2)*), and *stau-1(q798)* deletes double-stranded RNA-binding domain 4 (referred to as *stau-1(ΔdsRBD4)*). A peptide antibody was raised against double-stranded RNA-binding domain 4. *B*, quantitative RT-PCR results of *stau-1* mRNA expression during *C. elegans* development. mRNA levels were normalized according to total amount of RNA. *C*, Western blot using the STAU-1 peptide antibody on mixed stage lysate from wild-type, *stau-1(ΔdsRBD2)*, and *stau-1(ΔdsRBD4)* animals. The *stau-1* mutant lysates served as specificity controls. *In vitro* translated STAU-1 protein served as a positive control for the STAU-1 antibody. Tubulin served as a loading control. *Numbers* to the *left* indicate the approximate molecular mass in kDa according to the Fermentas PageRuler Plus Protein Ladder. *D*, Western blot using the STAU-1 peptide antibody on wild-type lysate from various developmental stages. *In vitro* translated STAU-1 protein served as a positive control for the STAU-1 antibody. Tubulin served as a loading control. Protein levels were normalized according to total amount of protein. *Error bars*, S.D.

phoretic mobility shift assays. We purified recombinant versions of STAU-1 mutant proteins, each with a single dsRBD deleted (supplemental Fig. S2). (ΔdsRBD2 protein was prone to aggregation and therefore was not pursued.) Each mutant protein bound DS3 dsRNA (Fig. 2*G*). ΔdsRBD3, -4, and -5 proteins bound with similar affinity as wild-type; only ΔdsRBD1 had a weaker affinity for the dsRNA, implying that it might contribute preferentially to RNA binding (Fig. 2*G*). However, we conclude that no single dsRBD is required for binding (although dsRBD2 could not be tested) and suggest that at least two STAU-1 dsRBDs normally bind dsRNA. These are the first tests of the binding properties of domain deletions in full-length Staufen protein.

Attempts to Examine the Biological Role of STAU-1—To attempt to examine the biological role of STAU-1, we first isolated and analyzed two genetic mutants that contain *stau-1* deletions. The *stau-1(tm2266)* mutant contains an in-frame deletion that removes dsRBD2, and *stau-1(q798)* contains an in-frame deletion that removes dsRBD4 (Fig. 3*A*). Henceforth, *stau-1(tm2266)* is referred to as *stau-1(ΔdsRBD2)*, and *stau-1(q798)* is referred to as *stau-1(ΔdsRBD4)*. *stau-1(ΔdsRBD2)* and *stau-1(ΔdsRBD4)* single mutants are homozygous viable and have no gross morphological defects. Because both mutations delete only one dsRBD, and no single dsRBD is required for RNA binding, these mutants probably are not null alleles.

We also attempted to analyze STAU-1 function via RNAi. Wild-type and both *stau-1* mutants were either fed or injected with dsRNA corresponding to four different regions of the *stau-1* transcript. In addition, we attempted RNAi in *eri-1(mg366)* mutants and animals expressing a *sid-1* transgene, backgrounds that both increase the efficiency of RNAi (53, 54). None of these methods significantly reduced the level of *stau-1* mRNA by qRT-PCR, so RNAi was not further pursued.

stau-1 Is Expressed Throughout Development—We next examined *stau-1* expression during development. We first analyzed its mRNA. Total RNA was extracted from wild-type animals at multiple developmental stages and used for qRT-PCR with primers specific to *stau-1* mRNA. *stau-1* mRNA was present during each stage of development (Fig. 3*B*). Embryos expressed more than twice as much *stau-1* mRNA compared with any other stage. All mRNA levels were normalized to the endogenous genes *ama-1* (RNA polymerase II) and *rps-25* (ribosomal subunit) (55, 56), which both produced RNAs that were constant at all stages of development.

STAU-1 protein levels were analyzed using an antibody raised against a 22-amino acid peptide within dsRBD4 (residues 500–521) (Fig. 3*A*). This antibody was specific for endogenous STAU-1 (Fig. 3*C*). In wild-type lysate, a single major band of ~85 kDa, similar to the predicted molecular mass of STAU-1 protein, was detected via Western analysis. In *stau-1(ΔdsRBD2)* lysate, the antibody detected a protein smaller than wild-type, indicative of a mutant protein. No protein was detected in *stau-1(ΔdsRBD4)* lysate because the target epitope is deleted in that mutant (Fig. 3*C*).

We used the STAU-1 antibody on proteins isolated from wild-type animals at each developmental stage and found that STAU-1 protein was expressed at similar levels (Fig. 3*D*). In comparison, *stau-1* mRNA was slightly more abundant in embryos than in later stages. However, both the protein and mRNA are present and persist throughout development.

Identification of STAU-1-associated mRNAs—To identify mRNAs physically associated with STAU-1, we immunoprecipitated endogenous STAU-1 from wild-type adult lysate (*WT IP*) and extracted the RNA, which was then linearly amplified and hybridized to Affymetrix *C. elegans* genome arrays for each of three biological replicas (Fig. 4*A*). For comparison, we used two controls: an IP with preimmune sera from wild-type adult lysate (*Preimmune IP*) and an IP with α-STAU-1 antibody from *stau-1(ΔdsRBD4)* adult lysate (*Mutant IP*; Fig. 4*A*). As expected, STAU-1 protein was immunoprecipitated only in the wild-type strain and only by the STAU-1 antibody (Fig. 4*B*).

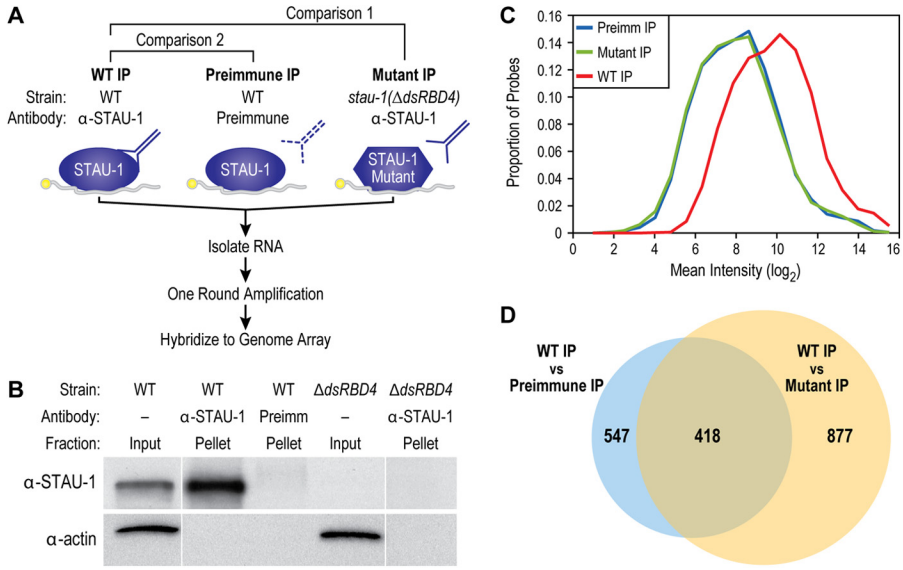

FIGURE 4. **RIP-Chip identifies endogenous STAU-1-associated mRNAs.** *A*, scheme for identification of STAU-1-associated mRNAs. α-STAU-1 antibody was used to immunoprecipitate endogenous STAU-1 from wild-type young adult lysate (*WT IP*). Two negative controls included immunoprecipitation using preimmune sera with wild-type young adult lysate (*Preimmune IP*) and immunoprecipitation using α-STAU-1 antibody with *stau-1(ΔdsRBD4)* young adult lysate (*Mutant IP*). RNA was isolated from the immunoprecipitations, linearly amplified, and hybridized to Affymetrix *C. elegans* genome arrays. The mRNAs associated with the WT IP were compared with those associated with the mutant IP (*Comparison 1*) and the Preimmune IP (*Comparison 2*) to identify STAU-1-associated mRNAs. *B*, Western analysis shows the α-STAU-1 antibody specifically immunoprecipitates STAU-1 protein from wild-type lysate (*lane 2*, *top*) but does not immunoprecipitate mutant protein (STAU-1(ΔdsRBD4)) in which the epitope is deleted (*lane 5*, *top*). STAU-1 protein is also not immunoprecipitated with preimmune serum (*lane 3*, *top*). α-STAU-1 antibody detects STAU-1 protein in the wild-type input (*lane 1*, *top*) but does not detect the mutant protein expressed in the *stau-1(ΔdsRBD4)* input (*lane 4*, *top*). α-Actin served as a loading control for the inputs (*lanes 1* and *4*, *bottom*). *C*, the log mean intensity for each microarray probe (*x* axis) was determined for preimmune IP (*blue line*), mutant IP (*green line*), and WT IP (*red line*) and plotted against the proportion of probes (*y* axis) with a given mean intensity. Overall, the WT IP has enriched signal intensity compared with the control IPs (*blue* and *green lines*). *D*, we compared WT IP with preimmune IP and compared WT IP with mutant IP and determined which transcripts had the highest SAM rank and were at least 4-fold enriched in the WT IP. Transcripts meeting these criteria from each comparison overlapped, resulting in 418 common STAU-1-associated mRNAs.

After normalization and log transformation (see "Experimental Procedures"), the mean signal intensity for each probe was plotted for all three samples. As expected, the WT IP sample exhibited an overall increase in mean signal intensity compared with the control IPs (Fig. 4*C*), suggesting an enrichment of RNA in the IP sample over the negative controls.

To determine which transcripts were reproducibly enriched in the WT IP sample compared with the control IPs, we analyzed our microarray data using the SAM program. SAM determines differential intensities between samples for each probe set by calculating a test statistic (SAM score) and false discovery rate (57). We used SAM for two comparisons: 1) WT IP *versus* mutant IP and 2) WT IP *versus* preimmune IP (Fig. 4*A*). Those transcripts that had the highest SAM score and were at least 4-fold enriched in the IP compared with the controls identified 1,295 transcripts for comparison 1 and 965 transcripts for comparison 2 (supplemental data sets 2 and 3). Overlap between the two sets resulted in 418 transcripts, which we deemed to be STAU-1-associated mRNAs (Fig. 4*D* and supplemental data set 1). By overlapping the two data sets, we may have discarded genuine STAU-1 targets, but we increased confidence that those we had identified were genuine. We considered that nonspecific association after lysis could result in mRNAs that would appear to be STAU-1 targets (58). To test this possibility computationally, we compared the list of 418 mRNAs with the 100 most abundant mRNAs present in wild-type young adults according to SAGE data (59). Only two STAU-1-associated transcripts were among the most highly expressed.

We next tested whether 10 transcripts enriched in the WT IP microarrays were also enriched by RT-PCR or qRT-PCR. As expected, each transcript was detected in the WT IP sample but was barely detectable in the control IPs (Fig. 5*A* and supplemental Fig. S4). M05B5.3 mRNA served as a negative control; it possesses predicted RNA secondary structure and was detected in the input samples but not in the IPs. The M05B5.3 transcript is a characterized target of the dsRNA-binding protein, ADAR (60). An abundant message, *act-1*, served as a loading control and positive control for the RT-PCR (Fig. 5*A*). Thus, these data validated the IP microarray findings. We conclude that the 418 transcripts comprise a likely set of RNAs associated with STAU-1.

We used DAVID to identify functional relationships among our list of STAU-1 associated mRNAs. DAVID offers functional annotation tools to identify biological themes or gene ontology (GO) terms from lists of genes (61). DAVID identified many biological themes among our list of STAU-1 targets. These included embryonic, larval, and reproductive development (Fig. 5*B* and supplemental data set 1). These are consistent with Staufen's previously characterized role in developmental patterning in *Drosophila* oocytes and embryos (32, 33, 62).

Comparison of Staufen-associated mRNAs Across Species—Furic *et al.* (42) identified transcripts associated with one isoform of human STAU1 (hSTAU1[55]) and two isoforms of human STAU2 (hSTAU2[59] and hSTAU2[62]). HA-tagged versions of all three proteins were transfected into HEK293T cells (naturally expressing STAU1 and STAU2 endogenously), and associated mRNAs were identified by RIP-Chip (42). Although

A

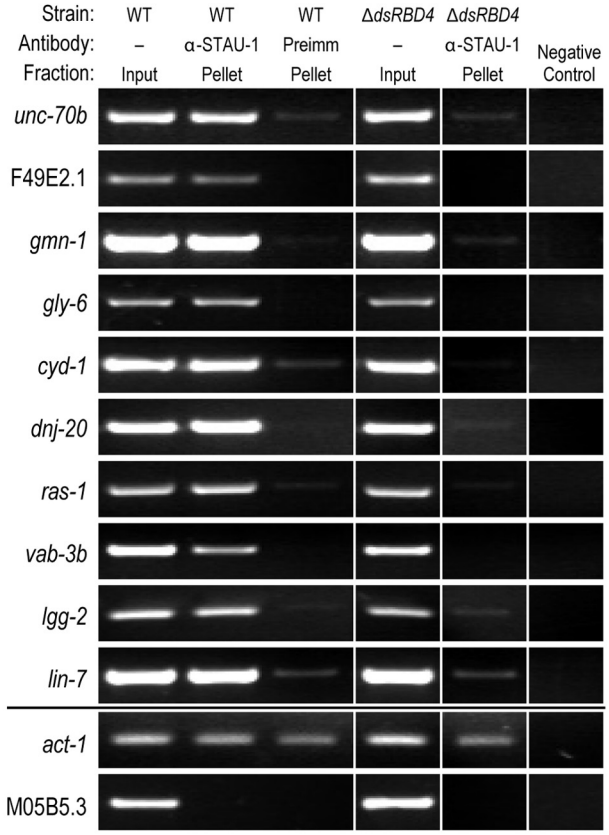

B DAVID terms associated with STAU-1 targets

Category	Term	Count	P value
Biological Process	GO:0009791 ~ post-embryonic development	105	7.22×10^{-10}
	GO:0002164 ~ larval development	102	4.56×10^{-9}
	GO:0009792 ~ embryonic development ending in birth or egg hatching	134	1.29×10^{-8}
	GO:0040007 ~ growth	82	7.77×10^{-8}
	GO:0040010 ~ positive regulation of growth rate	91	4.15×10^{-6}
	GO:0007548 ~ sex differentiation	49	2.07×10^{-5}
	GO:0003006 ~ reproductive developmental process	51	3.38×10^{-5}
	GO:0008104 ~ protein localization	24	7.66×10^{-4}
Cellular Compartment	GO:0005739 ~ mitochondrion	19	1.53×10^{-7}
	GO:0031090 ~ organelle membrane	15	2.15×10^{-5}

FIGURE 5. **IP RT-PCR validation of RIP-Chip results.** *A*, total RNA was isolated from immunoprecipitate inputs or pellets, reverse transcribed, and PCR-amplified using gene-specific primers. *act-1* served as a loading control. M05B5.3 is a transcript that did not appear on our list of STAU-1-associated mRNAs. Negative control samples did not contain any PCR template and control for DNA contamination. *B*, list of major DAVID terms associated with STAU-1 targets. *Count*, refers to the number of STAU-1 targets within each group.

all three human proteins are similar, they associated with distinct sets of mRNAs. Of the ~1,000 mRNAs associated with hSTAU1[55], several mRNAs were analyzed to identify a stem-loop similar to one within Arf1, a characterized hSTAU1 target. No stem-loop structure was identified, and no further analysis of RNA structure was pursued (42).

The STAU-1-associated mRNAs we identified do not overlap in a statistically significant fashion with those associated with human Staufen. Those instances of overlap we detect are compiled in supplemental Table S1. In addition, major GO terms associated with the human Staufen targets include cellular metabolism and cellular processes (42) and are not similar to the GO terms associated with *C. elegans* STAU-1 targets. We note that our studies analyzed STAU-1-associated RNAs in whole animals containing a wide array of cell types, whereas the human proteins were analyzed in a cultured cell line. Thus, the biological meaning of the apparent differences in the targets of the human and worm proteins is uncertain.

Structural Predictions Using STAU-1-associated mRNAs—Because STAU-1 preferentially bound dsRNA, we asked

whether the STAU-1-associated mRNAs possessed conspicuous structural elements. Most Staufen mRNA targets identified in other organisms require the 3′-UTR for Staufen association (5, 33, 36, 63). We analyzed all 3′-UTR sequences that were annotated (363 sequences) from our list of STAU-1-associated mRNAs, along with a random selection of *C. elegans* mRNAs, and folded the sequences using the Mfold structure prediction algorithm (64). Using the Gibbs free energy (ΔG) as a gauge for RNA secondary structure, we found that the 3′-UTRs of STAU-1-associated mRNAs contained more stable structures than the 3′-UTRs of a random set of mRNAs, and this difference was statistically significant (STAU-1 3′-UTRs, $\Delta G = -43.4$ kcal/mol; random 3′-UTRs, $\Delta G = -25.7$ kcal/mol; unpaired *t* test, $p < 0.0001$; supplemental data set 4). However, not all STAU-1-associated mRNAs contained dramatic structural elements in their 3′-UTRs. We also examined STAU-1-associated 5′-UTR sequences and detected no major structure. For those RNA targets that appear to lack structure, STAU-1 may bind via double-stranded structures outside the 5′- and 3′-UTR or via trans-acting RNA molecules. Alternatively, proteins bound to the RNA may recruit Staufen indirectly.

Effect of STAU-1 on Transgene Expression—While using transgene reporters to probe Staufen function, we observed effects on transgene expression. Mutants in the RNAi pathway, including *eri-1* and *rrf-3*, silence transgene expression (53, 65), and we observed a similar phenotype in both *stau-1* mutants. The *qIs43* reporter transgene is stably integrated in the genome and is linked to a *rol-6* dominant marker. The *rol-6* marker is a mutant form of the gene that is commonly used to identify animals that express the transgene because it causes animals to roll when they move (66). The *qIs43* transgene was crossed into *stau-1(ΔdsRBD2)* and *stau-1(ΔdsRBD4)* backgrounds to test whether STAU-1 affects transgene expression. We assayed the "rolling" phenotype of progeny from *stau-1* homozygotes, heterozygotes, and wild-type parents. 79–92% of progeny from wild-type strains containing the *qIs43* transgene have the "rolling" phenotype, indicative of transgene expression. However, only 2% of *stau-1(ΔdsRBD4)* and 38% of *stau-1(ΔdsRBD2*) animals exhibit the "rolling" phenotype (Table 1). Therefore, the *stau-1* mutations inhibited expression of the transgene as demonstrated by suppression of the *rol-6* marker. Because this transgene silencing phenotype is shared by mutants in the RNAi pathway, we pursued whether STAU-1 had any other connections to RNAi factors.

TABLE 1

***stau-1* mutants suppress transgene expression**

At least 20 animals were scored from each plate, and the roller phenotype was scored blindly, without regard to parental genotype.

Genotype of parent	Percentage of roller progeny[a]
	%
stau-1(ΔdsRBD4);qIs43	
ΔdsRBD4/ΔdsRBD4	2 ($n = 8$)
ΔdsRBD4/+	54 ($n = 13$)
+/+	92 ($n = 6$)
stau-1(ΔdsRBD2);qIs43	
ΔdsRBD2/ΔdsRBD2	38 ($n = 8$)
ΔdsRBD2/+	73 ($n = 11$)
+/+	79 ($n = 6$)

[a] *n* indicates the number of plates.

stau-1 Mutations Enhance Exogenous RNAi—To further examine the possible association between STAU-1 and RNAi, we compared the effect of *stau-1(ΔdsRBD2)* and *stau-1(ΔdsRBD4)* mutants on RNAi to those of *eri-1(mg366)*, a well characterized RNAi mutant. (ERI-1 protein is a ribonuclease in the endogenous RNAi pathway (50)). The *eri-1* mutation causes increased RNAi sensitivity when dsRNA is externally supplied and therefore displays an "enhancer of RNAi" phenotype (Eri). For example, *eri-1* mutations improve RNAi efficiency and lead to robust gene silencing and severe mutant phenotypes after exposure to exogenous RNAi (53). We tested the RNAi sensitivity of *stau-1(ΔdsRBD2)* and *stau-1(ΔdsRBD4*) animals by feeding the strains bacteria expressing *dpy-13* or *lir-1* dsRNA (53). Wild-type and *eri-1(mg366)* were used as controls.

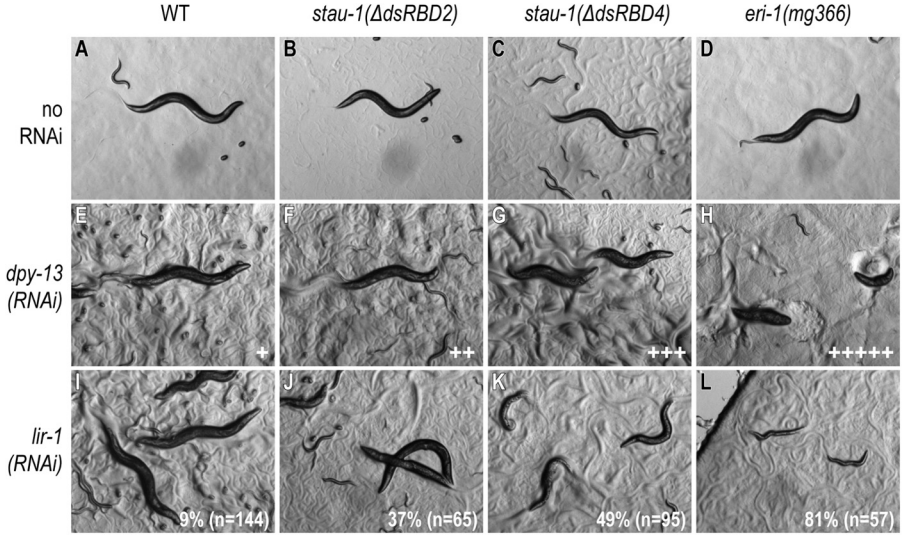

FIGURE 6. ***stau-1* mutations enhance exogenous RNAi.** Images represent the phenotypes of wild-type, *stau-1(ΔdsRBD2)*, *stau-1(ΔdsRBD4)*, and *eri-1(mg366*) animals after no RNAi (*A–D*), *dpy-13(RNAi*) (*E–H*), and *lir-1(RNAi*) (*I–L*). Both *stau-1(ΔdsRBD2*) and *stau-1(ΔdsRBD4*) exhibit enhanced RNAi phenotypes compared with wild-type. *eri-1(mg366*) was used as a positive control. *Plus signs* indicate the severity of the *dpy-13(RNAi*) phenotype: + indicates mildly dumpy, whereas +++++ indicates extremely dumpy. Percentages indicate the degree of lethality after *lir-1(RNAi*), and *n* signifies the number of total animals that were scored. Animals were considered "dead" if the pharynx was no longer pumping. Animals that no longer moved but still had a functioning pharynx were scored as "alive."

In *eri-1(mg366)* animals, *dpy-13(RNAi)* results in shortened body length (dumpy), and *lir-1(RNAi)* causes larval lethality. In contrast, wild-type animals subjected to *dpy-13(RNAi)* or *lir-1(RNAi*) are largely unaffected (53, 67). Both *stau-1* alleles displayed a more prominent dumpy phenotype than wild-type after *dpy-13(RNAi)*, although less extreme than with *eri-1(mg366)* (Fig. 6). Similarly, the *stau-1* alleles caused increased larval lethality after *lir-1(RNAi)* compared with wild-type but less than *eri-1* (wild-type = 9%, *stau-1(ΔdsRBD4)* = 49%, *stau-1(ΔdsRBD2)* = 37%, and *eri-1(mg366)* = 81% larval lethality; Fig. 6). In summary, we found that both *stau-1* mutant alleles are more sensitive to *dpy-13(RNAi)* and *lir-1(RNAi)* compared with wild-type. (The strains tested did not contain *mut-16* mutations, which are present in many "wild-type" *C. elegans* backgrounds and cause alterations in RNAi sensitivity (43).) These results suggest that mutations in *stau-1* enhance RNAi effectiveness and are therefore considered Eri.

stau-1(ΔdsRBD2);eri-1(mg366) Double Mutants Exhibit Synthetic Germ Line Defects—To test whether *stau-1* interacts genetically with *eri-1*, we crossed the *eri-1(mg366*) mutation into both *stau-1* mutant backgrounds. At 20°C, *eri-1(mg366)*, *stau-1(ΔdsRBD2)*, and *stau-1(ΔdsRBD4)* single mutants are self-fertile. The germ line morphology of *stau-1(ΔdsRBD2)* and *stau-1(ΔdsRBD4)* single mutants was similar to that of wild-type. However, we observed a small number of germ line abnormalities (7%) in *eri-1(mg366)* single mutants, which mostly consisted of unfertilized oocytes in the uterus (Fig. 7*B*). These results are consistent with earlier reports of defective sperm function associated with the *eri-1(mg366)* strain (67). Differential interference contrast microscopy of *stau-1(ΔdsRBD2);eri-1(mg366)* adults revealed severe defects, including uterine masses, abnormal oocyte morphology, and undefined or immature germ lines (Fig. 7*A*). Overall, 24.1% of gonad arms examined displayed an abnormality (Fig. 7*B*). However, only 3.7% of *stau-1(ΔdsRBD4);eri-1(mg366)* double mutants exhibited similar phenotypes (Fig. 7*B*). The disparate penetrance in the double mutants may reflect that the STAU-1 dsRBDs have slightly different functions. Nonetheless, *stau-1(ΔdsRBD2);eri-1(mg366*) mutants displayed germ line phenotypes that were distinct from either of the single mutants.

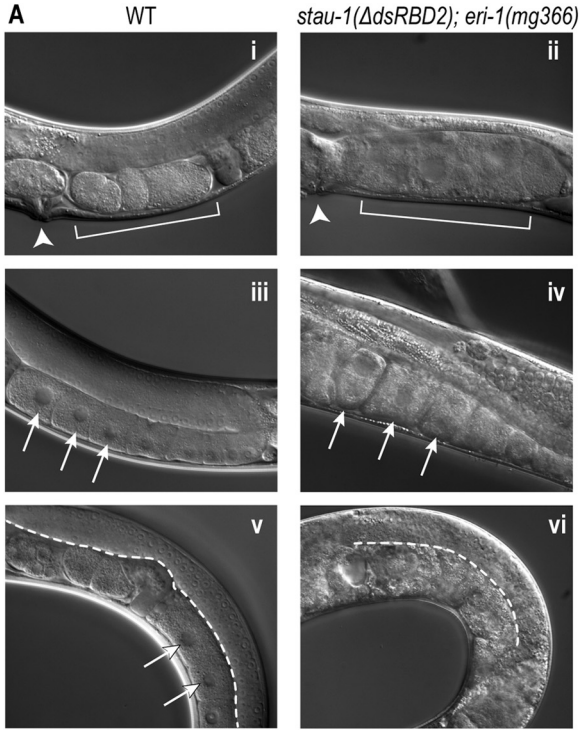

B

Strain	% abnormal	n (gonad arms)
WT	0	128
eri-1(mg366)	7.0	128
stau-1(ΔdsRBD4)	0	134
stau-1(ΔdsRBD2)	0.8	132
stau-1(ΔdsRBD4); eri-1(mg366)	3.7	136
stau-1(ΔdsRBD2); eri-1(mg366)	24.1	170

FIGURE 7. ***stau-1(ΔdsRBD2);eri-1(mg366)* exhibit synthetic germ line defects.** *A*, *stau-1(ΔdsRBD2);eri-1(mg366)* double mutants display defects, including uterine masses, abnormal oocytes, and undefined or immature germ lines when grown at 20°C. *Arrowheads* indicate the position of the vulva. *Brackets* indicate the uterus. *Arrows* point to oocytes. The *dotted line* denotes the compartmentalization of the germ line. In wild-type adults, the uterus contains embryos (*i*), whereas in some *stau-1(ΔdsRBD2);eri-1(mg366)* adults, the uterus is filled with an amorphous mass (*ii*). In wild-type adults, the oocytes are of uniform shape (*iii*), whereas some *stau-1(ΔdsRBD2);eri-1(mg366*) adult animals have misshapen oocytes (*iv*). The wild-type germ line is tubular and well structured (*v*), whereas some *stau-1(ΔdsRBD2);eri-1(mg366*) germ lines are immature and do not contain oocytes (*vi*). *B*, quantification of defects in single and double mutant strains. *n* indicates the number of gonad arms that were examined for each strain. Hermaphrodites possess two gonad arms.

DISCUSSION

We describe the biochemical and genetic characteristics of *C. elegans* STAU-1. Our studies establish that STAU-1 preferentially binds dsRNA with high affinity and that dsRBD1, -3, -4, and -5 are not required for binding RNA (ΔdsRBD2 could not be tested). The endogenous protein associates specifically with at least several hundred mRNAs. In addition, *stau-1* mutants exhibit phenotypes that suggest they affect the RNAi pathway.

Most protein-RNA analyses with dsRNA-binding proteins have focused on individual dsRBDs (4, 12), but analysis of intact protein allows a more comprehensive understanding of RNA specificity. Full-length STAU-1 bound dsRNA with high affinity and preferentially bound dsRNA (Fig. 2, *B–E*). Because full-length *Drosophila* Staufen is insoluble, its RNA binding has not been assayed *in vitro* (36). However, full-length human Staufen also appeared to discriminate RNA structure, not sequence (52). We find that full-length STAU-1 binds multiple double-stranded RNAs, with affinities that correlate well with the stability of the stem (Fig. 2*E*). In contrast, STAU-1 does not exhibit dramatic sequence specificity with single-stranded RNAs (Fig. 2*F*).

We found that at least two domains of STAU-1 probably bind dsRNA with high affinity, because deletion of any one dsRBD did not prevent dsRNA binding (Fig. 2*G*; domain 2 could not be tested). In *Drosophila* Staufen, domains 1, 3, and 4 bound dsRNA *in vitro*, whereas domains 2 and 5 did not (4). The analogous dsRBDs in STAU-1 may act similarly.

We identified mRNAs that associate with endogenous STAU-1 protein. Overall, our list of STAU-1-associated

mRNAs contains a statistically significant enrichment of structured RNAs compared with a random sample, although not all contained conspicuously structured 3′-UTRs (supplemental data set 4). Our RIP-Chip conditions did not require direct STAU-1-mRNA interactions, so we probably isolated direct as well as indirect protein-RNA complexes. Several Staufen mRNA targets that have been biologically validated do contain structured 3′-UTRs, such as *bicoid* from *Drosophila* and Arf1, a SMD target in mammals (5, 33). However, few Staufen-mRNA interactions have been verified *in vivo* (33, 36). Our results raise the possibility that a structured 3′-UTR may not be a requirement for Staufen association.

stau-1 mutants exhibit phenotypes that suggest STAU-1 impacts the RNAi pathway (Figs. 6 and 7). STAU-1 binds dsRNA of any sequence (Fig. 2*B*), and dsRNA is present at multiple steps during RNAi. ADAR is a dsRNA-binding protein that counteracts RNAi by binding and editing structured RNAi substrates (68). In plants, RNAi is used as an antiviral response, but plant viruses can temper this response by expressing dsRNA-binding proteins that sequester RNAi intermediates (69, 70). We suggest that although STAU-1 is not a primary component in RNAi, the overlap of a common substrate may cause alterations in the RNAi pathway in *stau-1*-defective animals. This may account for the transgene silencing (Table 1) and Eri phenotype (Fig. 6) associated with *stau-1* mutants. However, STAU-1(ΔdsRBD4) protein still binds RNA *in vitro* (Fig. 2*G*); thus, alterations in binding may not be responsible for the phenotypes associated with this genetic mutant.

We suggest three speculative possibilities for how STAU-1 may interact with those mRNAs that lack conspicuous secondary structures. First, STAU-1 may recognize secondary structures formed by more than one RNA molecule. For example, a *Drosophila* Staufen target, *bicoid*, contains a 3′-UTR that dimerizes to form more complex structures (35), and trans-acting RNAs nucleate assembly of mammalian STAU1 in one instance (71). Alternatively, Staufen could bind an imperfectly structured (or even single-stranded) RNA element that escaped our computational detection. Finally, STAU-1 may associate with mRNAs via protein partners. Further studies now are required to better understand how *C. elegans* STAU-1 associates with its RNA targets and to reveal the protein's biological consequences.

Acknowledgments—We thank the Kimble laboratory for advice, strains, and the use of microscopes. We also thank Aaron Kershner, Elena Sorokin, Kyung Won Kim, and Audrey Gasch for advice on microarray analysis. We thank the Kennedy laboratory for reagents and advice regarding RNAi assays. We are grateful to other members of the Wickens laboratory for advice and discussion. We thank the Barr laboratory for the C. elegans deletion library. We thank Laura Vanderploeg and the Biochemistry Media Laboratory for help with figures. We are grateful to the Caenorhabditis Genetic Center and the National Bioresource Project for nematode strains.

REFERENCES

1. Lunde, B. M., Moore, C., and Varani, G. (2007) RNA-binding proteins. Modular design for efficient function. *Nat. Rev. Mol. Cell Biol.* **8,** 479–490
2. Dreyfuss, G., Kim, V. N., and Kataoka, N. (2002) Messenger-RNA-binding proteins and the messages they carry. *Nat. Rev. Mol. Cell Biol.* **3,** 195–205
3. Roegiers, F., and Jan, Y. N. (2000) Staufen. A common component of mRNA transport in oocytes and neurons? *Trends Cell Biol.* **10,** 220–224
4. Micklem, D. R., Adams, J., Grünert, S., and St Johnston, D. (2000) Distinct roles of two conserved Staufen domains in oskar mRNA localization and translation. *EMBO J.* **19,** 1366–1377
5. Kim, Y. K., Furic, L., Desgroseillers, L., and Maquat, L. E. (2005) Mammalian Staufen1 recruits Upf1 to specific mRNA 3′UTRs so as to elicit mRNA decay. *Cell* **120,** 195–208
6. Saunders, L. R., and Barber, G. N. (2003) The dsRNA binding protein family. Critical roles, diverse cellular functions. *FASEB J.* **17,** 961–983
7. St Johnston, D., Brown, N. H., Gall, J. G., and Jantsch, M. (1992) A conserved double-stranded RNA-binding domain. *Proc. Natl. Acad. Sci. U.S.A.* **89,** 10979–10983
8. Chang, K. Y., and Ramos, A. (2005) The double-stranded RNA-binding motif, a versatile macromolecular docking platform. *FEBS J.* **272,** 2109–2117
9. Parker, G. S., Maity, T. S., and Bass, B. L. (2008) dsRNA binding properties of RDE-4 and TRBP reflect their distinct roles in RNAi. *J. Mol. Biol.* **384,** 967–979
10. Broadus, J., Fuerstenberg, S., and Doe, C. Q. (1998) Staufen-dependent localization of prospero mRNA contributes to neuroblast daughter-cell fate. *Nature* **391,** 792–795
11. Ryter, J. M., and Schultz, S. C. (1998) Molecular basis of double-stranded RNA-protein interactions. Structure of a dsRNA-binding domain complexed with dsRNA. *EMBO J.* **17,** 7505–7513
12. Ramos, A., Grünert, S., Adams, J., Micklem, D. R., Proctor, M. R., Freund, S., Bycroft, M., St Johnston, D., and Varani, G. (2000) RNA recognition by a Staufen double-stranded RNA-binding domain. *EMBO J.* **19,** 997–1009
13. Blaszczyk, J., Gan, J., Tropea, J. E., Court, D. L., Waugh, D. S., and Ji, X. (2004) Noncatalytic assembly of ribonuclease III with double-stranded RNA. *Structure* **12,** 457–466
14. Mueller, G. A., Miller, M. T., Derose, E. F., Ghosh, M., London, R. E., and Hall, T. M. (2010) Solution structure of the Drosha double-stranded RNA-binding domain. *Silence* **1,** 2
15. Fierro-Monti, I., and Mathews, M. B. (2000) Proteins binding to duplexed RNA. One motif, multiple functions. *Trends Biochem. Sci.* **25,** 241–246
16. Bernstein, E., Caudy, A. A., Hammond, S. M., and Hannon, G. J. (2001) Role for a bidentate ribonuclease in the initiation step of RNA interference. *Nature* **409,** 363–366
17. Hundley, H. A., and Bass, B. L. (2010) ADAR editing in double-stranded UTRs and other noncoding RNA sequences. *Trends Biochem. Sci.* **35,** 377–383
18. Hogg, M., Paro, S., Keegan, L. P., and O'Connell, M. A. (2011) RNA editing by mammalian ADARs. *Adv. Genet.* **73,** 87–120
19. Williams, B. R. (1999) PKR. A sentinel kinase for cellular stress. *Oncogene* **18,** 6112–6120
20. Meurs, E., Chong, K., Galabru, J., Thomas, N. S., Kerr, I. M., Williams, B. R., and Hovanessian, A. G. (1990) Molecular cloning and characterization of the human double-stranded RNA-activated protein kinase induced by interferon. *Cell* **62,** 379–390
21. Tabara, H., Yigit, E., Siomi, H., and Mello, C. C. (2002) The dsRNA binding protein RDE-4 interacts with RDE-1, DCR-1, and a DExH-box helicase to direct RNAi in *C. elegans*. *Cell* **109,** 861–871
22. Hartig, J. V., Esslinger, S., Böttcher, R., Saito, K., and Förstemann, K. (2009) Endo-siRNAs depend on a new isoform of loquacious and target artificially introduced, high-copy sequences. *EMBO J.* **28,** 2932–2944
23. Liu, Q., Rand, T. A., Kalidas, S., Du, F., Kim, H. E., Smith, D. P., and Wang, X. (2003) R2D2, a bridge between the initiation and effector steps of the *Drosophila* RNAi pathway. *Science* **301,** 1921–1925
24. Kok, K. H., Ng, M. H., Ching, Y. P., and Jin, D. Y. (2007) Human TRBP and PACT directly interact with each other and associate with dicer to facilitate the production of small interfering RNA. *J. Biol. Chem.* **282,** 17649–17657
25. Fire, A., Xu, S., Montgomery, M. K., Kostas, S. A., Driver, S. E., and Mello, C. C. (1998) Potent and specific genetic interference by double-stranded RNA in *Caenorhabditis elegans*. *Nature* **391,** 806–811
26. Mello, C. C., and Conte, D., Jr. (2004) Revealing the world of RNA inter-

ference. *Nature* **431,** 338–342
27. Sijen, T., and Plasterk, R. H. (2003) Transposon silencing in the *Caenorhabditis elegans* germ line by natural RNAi. *Nature* **426,** 310–314
28. Buchon, N., and Vaury, C. (2006) RNAi. A defensive RNA-silencing against viruses and transposable elements. *Heredity* **96,** 195–202
29. Wang, X. H., Aliyari, R., Li, W. X., Li, H. W., Kim, K., Carthew, R., Atkinson, P., and Ding, S. W. (2006) RNA interference directs innate immunity against viruses in adult *Drosophila*. *Science* **312,** 452–454
30. Schupbach, T., and Wieschaus, E. (1986) Germline autonomy of maternal-effect mutations altering the embryonic body pattern of Drosophila. *Dev. Biol.* **113,** 443–448
31. Lehmann, R., and Nüsslein-Volhard, C. (1991) The maternal gene nanos has a central role in posterior pattern formation of the *Drosophila* embryo. *Development* **112,** 679–691
32. St Johnston, D., Beuchle, D., and Nüsslein-Volhard, C. (1991) Staufen, a gene required to localize maternal RNAs in the *Drosophila* egg. *Cell* **66,** 51–63
33. Ferrandon, D., Elphick, L., Nüsslein-Volhard, C., and St Johnston, D. (1994) Staufen protein associates with the 3′UTR of bicoid mRNA to form particles that move in a microtubule-dependent manner. *Cell* **79,** 1221–1232
34. Li, P., Yang, X., Wasser, M., Cai, Y., and Chia, W. (1997) Inscuteable and Staufen mediate asymmetric localization and segregation of prospero RNA during *Drosophila* neuroblast cell divisions. *Cell* **90,** 437–447
35. Ferrandon, D., Koch, I., Westhof, E., and Nüsslein-Volhard, C. (1997) RNA-RNA interaction is required for the formation of specific bicoid mRNA 3′ UTR-STAUFEN ribonucleoprotein particles. *EMBO J.* **16,** 1751–1758
36. Schuldt, A. J., Adams, J. H., Davidson, C. M., Micklem, D. R., Haseloff, J., St Johnston, D., and Brand, A. H. (1998) Miranda mediates asymmetric protein and RNA localization in the developing nervous system. *Genes Dev.* **12,** 1847–1857
37. Köhrmann, M., Luo, M., Kaether, C., DesGroseillers, L., Dotti, C. G., and Kiebler, M. A. (1999) Microtubule-dependent recruitment of Staufen-green fluorescent protein into large RNA-containing granules and subsequent dendritic transport in living hippocampal neurons. *Mol. Biol. Cell* **10,** 2945–2953
38. Duchaîne, T. F., Hemraj, I., Furic, L., Deitinghoff, A., Kiebler, M. A., and DesGroseillers, L. (2002) Staufen2 isoforms localize to the somatodendritic domain of neurons and interact with different organelles. *J. Cell Sci.* **115,** 3285–3295
39. Mallardo, M., Deitinghoff, A., Müller, J., Goetze, B., Macchi, P., Peters, C., and Kiebler, M. A. (2003) Isolation and characterization of Staufen-containing ribonucleoprotein particles from rat brain. *Proc. Natl. Acad. Sci. U.S.A.* **100,** 2100–2105
40. Kiebler, M. A., Hemraj, I., Verkade, P., Kohrmann, M., Fortes, P., Marión, R. M., Ortín, J., and Dotti, C. G. (1999) The mammalian staufen protein localizes to the somatodendritic domain of cultured hippocampal neurons: implications for its involvement in mRNA transport. *J. Neurosci.* **19,** 288–297
41. Tang, S. J., Meulemans, D., Vazquez, L., Colaco, N., and Schuman, E. (2001) A role for a rat homolog of staufen in the transport of RNA to neuronal dendrites. *Neuron* **32,** 463–475
42. Furic, L., Maher-Laporte, M., and DesGroseillers, L. (2008) A genome-wide approach identifies distinct but overlapping subsets of cellular mRNAs associated with Staufen1- and Staufen2-containing ribonucleoprotein complexes. *RNA* **14,** 324–335
43. Zhang, C., Montgomery, T. A., Gabel, H. W., Fischer, S. E., Phillips, C. M., Fahlgren, N., Sullivan, C. M., Carrington, J. C., and Ruvkun, G. (2011) mut-16 and other mutator class genes modulate 22G and 26G siRNA pathways in *Caenorhabditis elegans*. *Proc. Natl. Acad. Sci. U.S.A.* **108,** 1201–1208
44. Chien, C. T., Bartel, P. L., Sternglanz, R., and Fields, S. (1991) The two-hybrid system. A method to identify and clone genes for proteins that interact with a protein of interest. *Proc. Natl. Acad. Sci. U.S.A.* **88,** 9578–9582
45. Hook, B., Bernstein, D., Zhang, B., and Wickens, M. (2005) RNA-protein interactions in the yeast three-hybrid system. Affinity, sensitivity, and enhanced library screening. *RNA* **11,** 227–233
46. Bernstein, D., Hook, B., Hajarnavis, A., Opperman, L., and Wickens, M. (2005) Binding specificity and mRNA targets of a *C. elegans* PUF protein, FBF-1. *RNA* **11,** 447–458
47. Campbell, Z. T., Bhimsaria, D., Valley, C. T., Rodriguez-Martinez, J. A., Menichelli, E., Williamson, J. R., Ansari, A. Z., and Wickens, M. (2012) Cooperativity in RNA-protein interactions. Global analysis of RNA binding specificity. *Cell Rep.* **1,** 570–581
48. Schmittgen, T. D., and Livak, K. J. (2008) Analyzing real-time PCR data by the comparative C(T) method. *Nat. Protoc.* **3,** 1101–1108
49. Timmons, L., Court, D. L., and Fire, A. (2001) Ingestion of bacterially expressed dsRNAs can produce specific and potent genetic interference in *Caenorhabditis elegans*. *Gene* **263,** 103–112
50. Gent, J. I., Lamm, A. T., Pavelec, D. M., Maniar, J. M., Parameswaran, P., Tao, L., Kennedy, S., and Fire, A. Z. (2010) Distinct phases of siRNA synthesis in an endogenous RNAi pathway in *C. elegans* soma. *Mol. Cell* **37,** 679–689
51. Welker, N. C., Pavelec, D. M., Nix, D. A., Duchaine, T. F., Kennedy, S., and Bass, B. L. (2010) Dicer's helicase domain is required for accumulation of some, but not all, *C. elegans* endogenous siRNAs. *RNA* **16,** 893–903
52. Wickham, L., Duchaîne, T., Luo, M., Nabi, I. R., and DesGroseillers, L. (1999) Mammalian staufen is a double-stranded-RNA- and tubulin-binding protein which localizes to the rough endoplasmic reticulum. *Mol. Cell Biol.* **19,** 2220–2230
53. Kennedy, S., Wang, D., and Ruvkun, G. (2004) A conserved siRNA-degrading RNase negatively regulates RNA interference in *C. elegans*. *Nature* **427,** 645–649
54. Calixto, A., Chelur, D., Topalidou, I., Chen, X., and Chalfie, M. (2010) Enhanced neuronal RNAi in *C. elegans* using SID-1. *Nat. Methods* **7,** 554–559
55. Cui, M., Kim, E. B., and Han, M. (2006) Diverse chromatin remodeling genes antagonize the Rb-involved SynMuv pathways in *C. elegans*. *PLoS Genet.* **2,** e74
56. Pohludka, M., Simeckova, K., Vohanka, J., Yilma, P., Novak, P., Krause, M. W., Kostrouchova, M., and Kostrouch, Z. (2008) Proteomic analysis uncovers a metabolic phenotype in *C. elegans* after nhr-40 reduction of function. *Biochem. Biophys. Res. Commun.* **374,** 49–54
57. Tusher, V. G., Tibshirani, R., and Chu, G. (2001) Significance analysis of microarrays applied to the ionizing radiation response. *Proc. Natl. Acad. Sci. U.S.A.* **98,** 5116–5121
58. Mili, S., and Steitz, J. A. (2004) Evidence for reassociation of RNA-binding proteins after cell lysis. Implications for the interpretation of immunoprecipitation analyses. *RNA* **10,** 1692–1694
59. McKay, S. J., Johnsen, R., Khattra, J., Asano, J., Baillie, D. L., Chan, S., Dube, N., Fang, L., Goszczynski, B., Ha, E., Halfnight, E., Hollebakken, R., Huang, P., Hung, K., Jensen, V., Jones, S. J., Kai, H., Li, D., Mah, A., Marra, M., McGhee, J., Newbury, R., Pouzyrev, A., Riddle, D. L., Sonnhammer, E., Tian, H., Tu, D., Tyson, J. R., Vatcher, G., Warner, A., Wong, K., Zhao, Z., and Moerman, D. G. (2003) Gene expression profiling of cells, tissues, and developmental stages of the nematode *C. elegans*. *Cold Spring Harb. Symp. Quant. Biol.* **68,** 159–169
60. Morse, D. P., Aruscavage, P. J., and Bass, B. L. (2002) RNA hairpins in noncoding regions of human brain and *Caenorhabditis elegans* mRNA are edited by adenosine deaminases that act on RNA. *Proc. Natl. Acad. Sci. U.S.A.* **99,** 7906–7911
61. Dennis, G., Jr., Sherman, B. T., Hosack, D. A., Yang, J., Gao, W., Lane, H. C., and Lempicki, R. A. (2003) DAVID. Database for Annotation, Visualization, and Integrated Discovery. *Genome Biol.* **4,** P3
62. van Eeden, F., and St Johnston, D. (1999) The polarisation of the anterior-posterior and dorsal-ventral axes during Drosophila oogenesis. *Curr. Opin. Genet. Dev.* **9,** 396–404
63. Kim, Y. K., Furic, L., Parisien, M., Major, F., DesGroseillers, L., and Maquat, L. E. (2007) Staufen1 regulates diverse classes of mammalian transcripts. *EMBO J.* **26,** 2670–2681
64. Zuker, M. (2003) Mfold web server for nucleic acid folding and hybridization prediction. *Nucleic Acids Res.* **31,** 3406–3415
65. Simmer, F., Tijsterman, M., Parrish, S., Koushika, S. P., Nonet, M. L., Fire, A., Ahringer, J., and Plasterk, R. H. (2002) Loss of the putative RNA-

directed RNA polymerase RRF-3 makes *C. elegans* hypersensitive to RNAi. *Curr. Biol.* **12,** 1317–1319
66. Mello, C. C., Kramer, J. M., Stinchcomb, D., and Ambros, V. (1991) Efficient gene transfer in C. elegans. Extrachromosomal maintenance and integration of transforming sequences. *EMBO J.* **10,** 3959–3970
67. Pavelec, D. M., Lachowiec, J., Duchaine, T. F., Smith, H. E., and Kennedy, S. (2009) Requirement for the ERI/DICER complex in endogenous RNA interference and sperm development in *Caenorhabditis elegans*. *Genetics* **183,** 1283–1295
68. Wu, D., Lamm, A. T., and Fire, A. Z. (2011) Competition between ADAR and RNAi pathways for an extensive class of RNA targets. *Nat. Struct. Mol. Biol.* **18,** 1094–1101
69. Nakahara, K. S., Masuta, C., Yamada, S., Shimura, H., Kashihara, Y., Wada, T. S., Meguro, A., Goto, K., Tadamura, K., Sueda, K., Sekiguchi, T., Shao, J., Itchoda, N., Matsumura, T., Igarashi, M., Ito, K., Carthew, R. W., and Uyeda, I. (2012) Tobacco calmodulin-like protein provides secondary defense by binding to and directing degradation of virus RNA silencing suppressors. *Proc. Natl. Acad. Sci. U.S.A.* **109,** 10113–10118
70. Mérai, Z., Kerényi, Z., Kertész, S., Magna, M., Lakatos, L., and Silhavy, D. (2006) Double-stranded RNA binding may be a general plant RNA viral strategy to suppress RNA silencing. *J. Virol.* **80,** 5747–5756
71. Gong, C., and Maquat, L. E. (2011) lncRNAs transactivate STAU1-mediated mRNA decay by duplexing with 3′-UTRs via Alu elements. *Nature* **470,** 284–288
72. Hofacker, I. L. (2003) Vienna RNA secondary structure server. *Nucleic Acids Res.* **31,** 3429–3431